



A mathematical model for aeolian megaripples on Mars

H. Yizhaq*

BIDR, Ben Gurion University, Sede Boker Campus 84990, Israel

Available online 22 June 2005

Abstract

The recent mathematical model for megaripples formation proposed by Yizhaq [Physica A 338 (2004) 211] is used to explain the huge megaripples formation observed on Mars. The model also predicts a few linearly unstable modes which correspond to megaripples with different wavelengths at the same wind condition as seen in some places on Mars. Studying these aeolian bedforms can provide information about the past and present climatic conditions on Mars.

© 2005 Elsevier B.V. All rights reserved.

Keywords: Sand ripples; Megaripples; Saltation; Reptation; Mars

1. Introduction

Megaripples are ubiquitous in most of the aeolian sand deposits of the world. Compared to ordinary wind ripples, megaripples are much larger, more prominent and vary considerably in appearance. Megaripple wavelengths vary between 30 and 2000 cm with a height of up to 100 cm. Aeolian processes are known to occur on Mars today and include dust storm, dust devils, dunes and megaripples. Megaripples on Mars exhibit much longer dimensions [2–4]. The Mars Orbiter Camera (MOC) from the Mars Global Surveyor has provided new high-resolution images (see Fig. 1) of aeolian bedforms including small transverse dunes or large aeolian megaripples

*Fax: +972 8 6596921.

E-mail address: yiyeh@bgumail.bgu.ac.il.

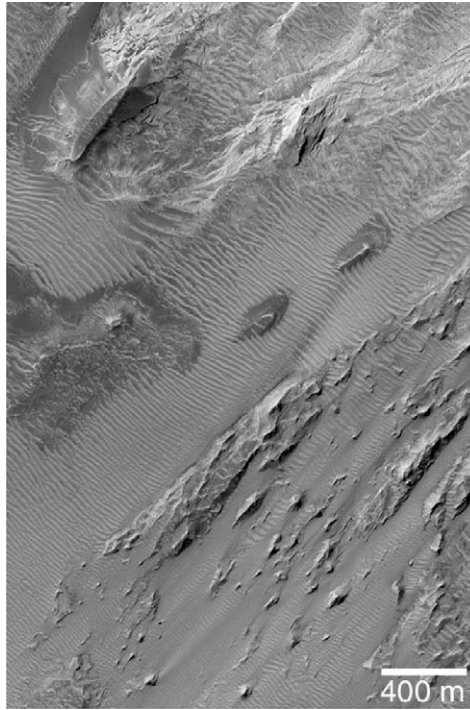


Fig. 1. A Mars Orbiter Camera (MOC) image showing the plethora of large, aeolian ripples among wind-sculpted sedimentary rocks in eastern Candor Chasma. Candor Chasma is one of the troughs of the Valles Marineris, a system of chasms that would stretch all the way across North America if it were on Earth. This picture is located near 7.9°S , 64.9°W . Sunlight illuminates the scene from the left/upper left. Image credit: NASA/JPL/Malin Space Science Systems.

with wavelengths of 10–60 m and heights from a few to 10 m. Most of these bedforms occur in troughs, pits, craters and on deflated plains [5]. The newly discovered Martian bedforms are distinct from known bedforms on Earth, as their scale is between the scale of megaripples and that of small dunes. Recently [6], megaripples with a wavelength of 38 m were measured, using stereo-images from the Mars Orbiter Camera onboard the Mars Global Surveyor, to have heights of 5.7 m which give a ripple index of 6.7, much lower than that of terrestrial megaripples which is about 15. These huge Martian megaripples may be a result of the lower Martian gravity and the higher overall windspeeds required for saltation¹ in the low-density atmosphere which leads to a greatly increased saltation length [9,10]. Owen [11]

¹According to Greeley et al. [7], extrapolation to the low-density CO_2 atmosphere of Mars shows that the minimum frictional velocities to set sand into saltation is 10 times greater than on Earth. In turn, this leads to particle velocities which are some three times greater than on Earth depending on the surface roughness [8].

computed the saltation length on Mars and predicted it to be 41.7 m. Another value which is used in the literature is 12.5 m [12], but more data are needed in order to confirm these estimations. Because the trajectories are long, the incidence angles of the impacting saltation particles should be lower than those on Earth [11]. Terrestrial megaripples are known to have distinctly bi- or multi-modal grain sizes which are vertically segregated by wind action. It is still unknown whether the Martian features also involve a bimodal distribution of grain particles like megaripples on Earth and it is hoped that the Mars Exploration rovers, Spirit and Opportunity, will take a closer look at the newly observed large bedforms and thus shed light on their formation.

In this study, I apply the recent minimal mathematical model for aeolian megaripples formation [1], which is an extension of the normal sand ripples model [13], in the context of the Martian megaripple. Linear stability analysis indicates the presence of several maxima in the growth rate curves, which correspond to megaripples with different wavelengths. The model is regarded minimal as it does not explicitly describe the dynamics of the vertical segregation between coarse and fine grains for the nascent ripples, as well as the feedback of the bedform on the sand flux.

2. Brief description of the model

The main assumption of the model is that the sediment consists of a mixture of grains with two different sizes and that the wind is not strong enough to cause saltation of the coarse grains. Only fine grains saltate and drive the coarse grains into reptation (for details of the model see [1]). The Exner equation which expresses the conservation of mass includes spatial variations of both reptation and saltation fluxes. The model adopts the following integro-differential equation:

$$\zeta_t = -Q_0 \partial_x \left\{ \varepsilon(1 - \mu_s) \int_{-\infty}^{\infty} p_{st}(\beta) d\beta \int_{x-\beta}^x F(x') dx' + n_p \delta(1 - \mu_r) \int_0^{\infty} p_{rc}(\alpha) d\alpha \int_{x-\alpha}^x F(x') dx' \right\}, \tag{1}$$

where

$$Q_0 = N_{im}^0 m_f \cot \phi / [\rho_p(1 - \lambda_p)] \quad \text{and} \quad F(x) = \frac{\text{Max}(\tan \phi + \zeta_x, 0)}{\sqrt{1 + \zeta_x^2}}. \tag{2}$$

The probability distribution of the saltation and reptation fluxes are, respectively, defined as

$$p_{st}(\beta) = A \exp[(\beta - b)/(2\sigma^2)], \quad p_{rc}(\alpha) = \frac{1}{a} \exp(-\alpha/a). \tag{3}$$

The different parameters which are used in the model are summarized in Table 1. As the integro-differential model (Eq. 1) consists of two space integrals, its numerical solution demands several computing resources. Fig. 2 shows the time evolution of

Table 1
Definition of the main model quantities (discussed in detail in [1])

λ_p	Bed Porosity (typically taken as 0.35).
ρ_p	Grain density.
m_c	Coarse grain mass.
m_f	Fine grain mass.
ε	The ratio between coarse and fine sand at the bed surface.
δ	m_c/m_f ($27 \leq \delta \leq 343$).
n_p	Number of ejecting coarse grains per one saltation impact.
μ_r	Reptation length slope modification coefficient.
μ_s	Saltation length slope modification coefficient.
p_{rc}	Probability distribution of coarse reptation flux (exponential).
p_{sf}	Probability distribution of fine saltation flux (Gaussian).
σ	p_{sf} standard deviation.
A	Normalization constant: $A = 1/(\sigma\sqrt{2\pi})$.
N_{im}	Number density of impacting grains on an inclined surface.
N_{im}^0	Number density of impacting grains on a flat surface ($\sim 10^7$).
θ	Bed inclination.
ϕ	Descending angle of saltating grains.
a	Mean reptation hop length.
b	Mean saltation hop length.

incipient megaripples for the first 13 min. Megaripples start as normal ripples as was observed in the field by Murray [14]. The ripples wavelength increases in time due to merging of smaller ripples and the growth rate of the ‘megaripple’ mode is very small. It remains for future work to understand as to what determines the megaripple crest to crest spacings. The first hypothesis follows Ellwood et al. [17] which states that the large wavelength reflects an inherent length scale related to the characteristic saltation length of the fine fraction (the parameter b in the model). In an alternative hypothesis applicable to many different kinds of bedforms, the wavelength tends to increase in time, often through bedform mergers [18]. In this hypothesis, the wavelength observed in nature reflects the length of time over which the pattern has been developed, and the availability of ‘defects’ or imperfections in bedform crests that facilitate merging of individual crests. In this scenario, the large wavelength of megaripples, relative to the normal ripples, mainly reflects a longer lifetime for megaripples, whose crests are armored by coarse grains.

3. Modeling Martian megaripples

Assuming that the same mechanism for megaripples formation is also active on Mars, the model described in Section 2 can be used to predict the fastest growing wavelengths, although there is a large uncertainty concerning the values of the basic model parameters like the mean saltation path. Fig. 3 shows the growth rate curves²

²For details of the linear stability analysis, see [1].

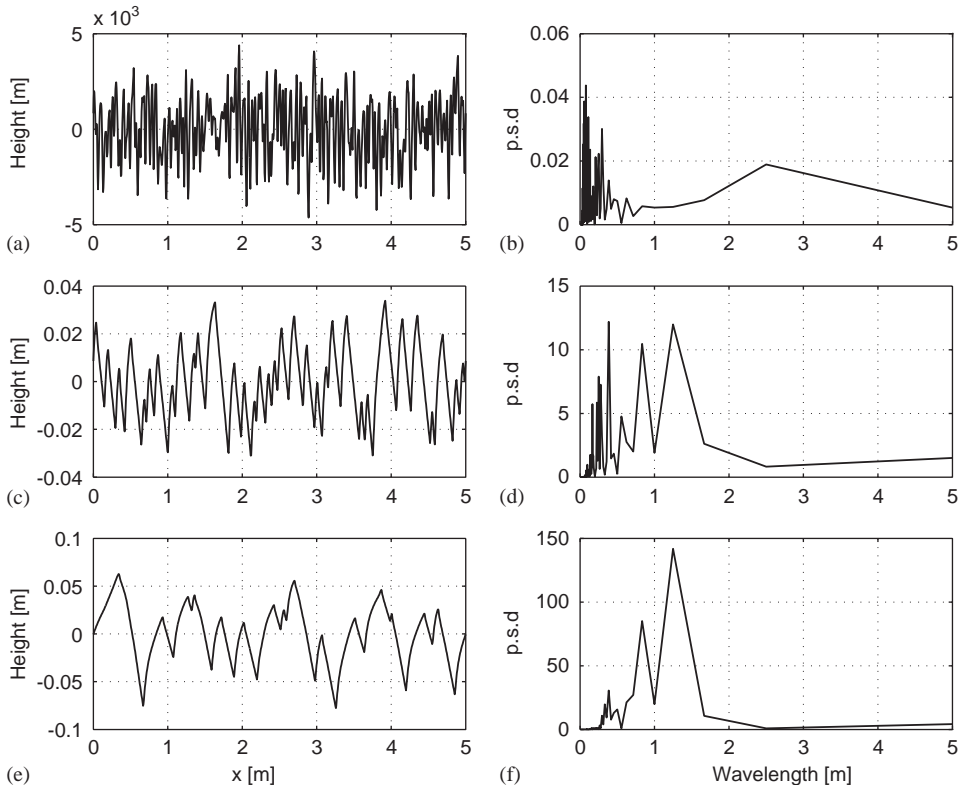


Fig. 2. Numerical solutions of the model equation (Eq. 1) at times (a) 5 s, (b) 305 s, and (c) 800 s and the corresponding power spectrum density (the mean of the Fourier transform squared amplitudes) plots (b), (d) and (f), respectively. The megaripples start as normal ripples and then the coarsening process takes place. It can be seen that after 13 min, the mode with wavelength 1.25 m becomes more prominent and the ripples height is ~ 10 cm. These results confirm Murray’s observation [14] from Morocco that after 1 day of strong wind, megaripples of 1 m wavelength were observed. The incipient megaripples developed from random perturbations of a flat bed and periodic boundary conditions were used. Note the different vertical scales used in drawing the ripples profiles. Parameters: $b = 0.4$ m, $a = 0.5$ cm, $n_p = 1$, $\phi = 10^\circ$, $\delta = 27$, $\mu_r = 0.4$, $\mu_s = 0.2$, fine grain diameter 0.25 mm.

of infinitesimal perturbations, for $b = 12$ m, $a = 0.1$ cm and $\sigma = 5$ m (solid line). From this, we obtain megaripples with $\lambda = 64$ m. For the same choice of b and a but with $\sigma = 2$ m, the growth curve has two maxima (dashed line) related to wavelengths of 64 m and 12.5 m, respectively. Megaripples of several wavelengths were observed at several locations on Mars (cf. Fig. 5 in [15]). These results indicate that a distribution of saltation lengths with a lower standard deviation predicts a few linearly unstable modes.

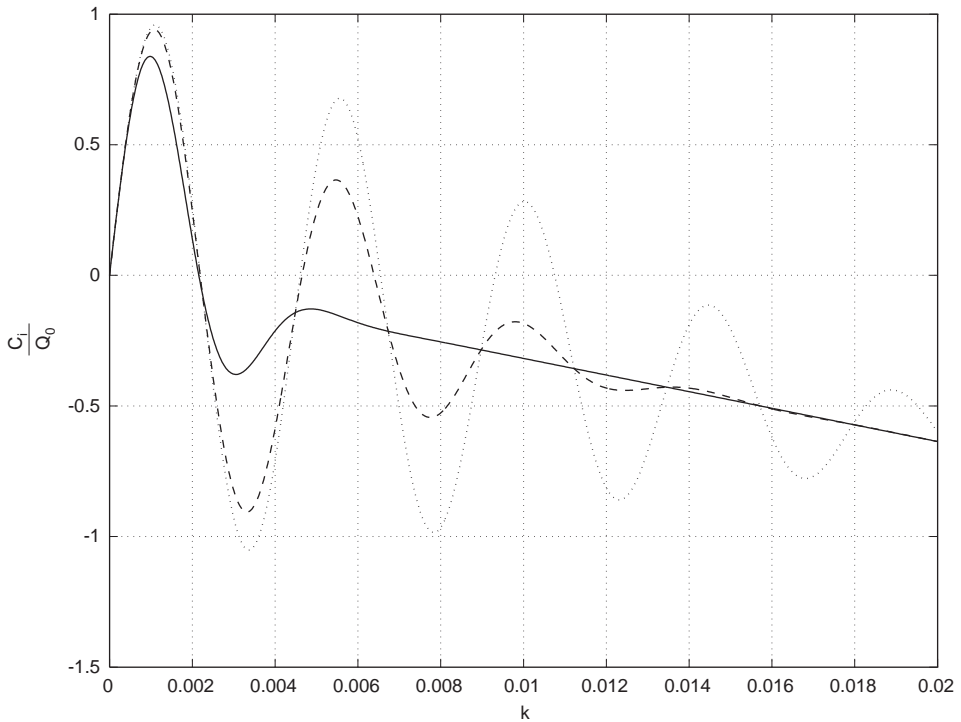


Fig. 3. Dispersion relations, i.e., perturbation growth rate vs. wave number. Positive growth rates indicate unstable modes. For $\sigma = 5$ m (solid line), the maximum corresponds to a wavelength of 64 m and for $\sigma = 2$ m (dashed line), there are two maxima corresponding to wavelengths of 64 and 12.5 m, respectively. In addition to the former two modes, a third mode becomes unstable for $\sigma = 1$ m (dotted line), with a wavelength of 6.28 m. Other parameters values: $\varepsilon = 1$, $b = 14$ m, $a = 0.1$ cm, $\phi = 7^\circ$, $\delta = 27$, $n_p = 1$.

4. Conclusions

Numerical results of the recent model presented by Yizhaq [1] show that megaripples start as normal ripples and the mode which corresponds to the larger wavelength slowly grows as more small ripples coalesce. The proposed model gives one possible mechanism for the formation of the recently large Martian bedforms. Linear stability analysis predicts that large ripples with wavelengths of tens of meters can grow if the basic mechanism for megaripple formation is the same as on Earth and if the mean saltation length is of an order of 10 m. Solving the model for a large space domain and for a longer time is needed to explain the larger height of the megaripples. More reliable data on Earth and Mars aeolian activity will provide more accurate estimations of the main parameters used in the model. We leave these two directions of research for future studies.

Acknowledgements

I wish to thank to Brad Murray for sharing with me his preliminary experimental results from the Moroccan Sahara.

References

- [1] H. Yizhaq, *Physica A* 338 (2004) 211.
- [2] K.S. Edgett, *Lunar Planet. Sci.* XXXII (2001) 1181.pdf.
- [3] J.R. Zimbelman, S. Wilson, *Lunar Planet. Sci.* XXXIII (2001) 1514.pdf.
- [4] S.A. Wilson, J.R. Zimbelman, S.H. Williams, *Lunar Planet. Sci.* XXXIV (2003) 1862.pdf.
- [5] K. S. Edgett, Abstract submitted to the GSA Annual Meeting, 5–8 November, 2001.
- [6] K.K. Williams, J.R. Zimbelman, *GSA Abstract with Program*, vol. 35, no. 6, 2003, p. 67.
- [7] R. Greeley, R.O. Kuzmin, R.M. Haberle, *Space Sci. Rev.* 96 (2002) 393.
- [8] R. Greeley, *Plant. Space Sci.* 50 (2002) 151.
- [9] B.R. White, *J. Geophys. Res.* 84 (1979) 4643.
- [10] R. Greeley, et al., *J. Geophys. Res.* 107 (E1) (2002).
- [11] R. Greeley, J. Iversen, *Wind as a Geological Process*, Cambridge University Press, Cambridge 1985.
- [12] C.D. Cooper, J.F. Mustard, *Lunar Planet. Sci.* XXIX (1998), no. 1164. University Press, New York, 1985.
- [13] H. Yizhaq, et al., *Physica D* 195 (2004) 207.
- [14] A.B. Murray, Private communication, 2004.
- [15] S.H. Williams, et al., *Lunar Planet. Sci.* XXXIII (2002) 1508.pdf.
- [17] J.M. Ellwood, et al., *J. Sedimentol. Petrol.* 45 (1975) 554.
- [18] A.B. Murray, *Geophys. Monogr.* 135 (2003) 151.